

Article

Electroless Platinum Deposition Using $\text{Co}^{3+}/\text{Co}^{2+}$ Redox Couple as a Reducing Agent

Loreta Tamasauskaite-Tamasiunaite ^{1,*} , Yezdi Dordi ², Eugenijus Norkus ¹, Ina Stankeviciene ¹, Aldona Jagminiene ¹, Arnas Naujokaitis ¹, Liudas Tumonis ³, Vytenis Buzas ³ and Laurynas Maciulis ³

¹ Center for Physical Sciences and Technology, Saulėtekio Ave. 3, LT-10257 Vilnius, Lithuania; eugenijus.norkus@ftmc.lt (E.N.); ina.stankeviciene@ftmc.lt (I.S.); aldona.jagminiene@ftmc.lt (A.J.); arnas.naujokaitis@ftmc.lt (A.N.)

² Lam Research Corporation, Fremont, CA 94538, USA; yezdi.dordi@lamresearch.com

³ NanoAvionics, JSC, Mokslininkų Str. 2A, LT-08412 Vilnius, Lithuania; liudas.tumonis@gmail.com (L.T.); vytenis@nanoavionics.com (V.B.); laurynas.maciulis@vgtu.lt (L.M.)

* Correspondence: loreta.tamasauskaite@ftmc.lt

Abstract: In the present work, the kinetics of electroless deposition of Pt, using a cobalt ion redox system ($\text{Co}^{3+}/\text{Co}^{2+}$) as a reducing agent, has been investigated. The deposition rate of Pt depends on the pH, concentration of reactants, and temperature. The deaeration and bubbling of the plating solution with argon play an essential role. It was found that 0.11 mg cm^{-2} of Pt films could be deposited on the surface of a roughed glass sheet in one hour without replenishing the solution. Additional data have been obtained on the grounds of electrochemical quartz crystal microbalance experiments. The bubbling (agitation) of the electroless Pt plating solution with argon during the deposition of Pt results in a higher deposition rate and is ca. $3 \mu\text{g cm}^{-2} \text{ min}^{-1}$. The Pt deposition rate is far less, and is as low as $0.14 \mu\text{g cm}^{-2} \text{ min}^{-1}$ when the electroless Pt plating solution is not bubbled with argon during the deposition of Pt.

Keywords: platinum; cobalt; electroless deposition; EQCM



Citation: Tamasauskaite-Tamasiunaite, L.; Dordi, Y.; Norkus, E.; Stankeviciene, I.; Jagminiene, A.; Naujokaitis, A.; Tumonis, L.; Buzas, V.; Maciulis, L. Electroless Platinum Deposition Using $\text{Co}^{3+}/\text{Co}^{2+}$ Redox Couple as a Reducing Agent.

Materials **2021**, *14*, 1893. <https://doi.org/10.3390/ma14081893>

Academic Editors: X. Ramón Nóvoa and Masato Sone

Received: 24 February 2021

Accepted: 8 April 2021

Published: 10 April 2021

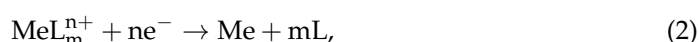
Publisher's Note: MDPI stays neutral with regard to jurisdictional claims in published maps and institutional affiliations.



Copyright: © 2021 by the authors. Licensee MDPI, Basel, Switzerland. This article is an open access article distributed under the terms and conditions of the Creative Commons Attribution (CC BY) license (<https://creativecommons.org/licenses/by/4.0/>).

1. Introduction

Nowadays, electroless metal plating processes are applied in many areas of research and industry, e.g., in metallization, galvanoplastic, microcircuits, and optoelectronics. Moreover, they are successfully used to form catalysts for fuel cells and in various catalytic processes, such as catalytic steam methane reforming (SMR), methanol oxidation, etc. [1–9]. In general, the mechanism of electroless metal deposition (Equation (1)) is considered as the coupling of the cathodic reaction of reducing of metal ions (Equation (2)) and the anodic reaction of oxidation of the reducing agent (Equation (3)), occurring simultaneously at the surface to be plated:



Therefore, under open-circuit conditions, an electrode attains a mixed potential (E_m) due to both partial reactions (Equations (2) and (3)) occurring at equal rates [10–13].

A sufficiently strong reducing agent is required for autocatalytic metal deposition. The use of traditional reducing agents, such as borohydride, borane dimethylamine, and hypophosphite, results in the deposition of non-pure metal coatings that contained boron or phosphorous [14–16]. Moreover, when using hydrogen-containing reducing agents, the deposited coating structure has large defects due to the evolution of hydrogen gas. The use of hydrogen-containing reducing agents is also connected with environmental and technological problems: (1) the plating bath cannot be recycled, i.e., the reducing agent

oxidizes irreversibly; (2) formaldehyde and most ligands are environmentally unacceptable; and (3) the plating rate and solution stability are not high enough. The search for new types of solutions, which would be more environmentally-friendly and have a higher plating rate and solution stability, has been made in some works [17,18]. For the reasons mentioned above, the search for and investigations of new reducing agents, e.g., charge-transfer reducers, *viz.* the different oxidation state metal-ion redox couples, are ongoing. In this case, multivalent metal ions with lower oxidation states are strong enough to reduce other metal ions to metallic states: Cr^{2+} , Cr^{3+} , Ti^{2+} , Ti^{3+} , V^{2+} , V^{3+} , V^{4+} , Cu^+ , Sn^{2+} , Fe^{2+} . Generally, the most pronounced catalytic effect has been observed for the $\text{Co}^{3+}/\text{Co}^{2+}$ redox couple. For the first time, the use of Co^{2+} complexes with ethylenediamine as reducing agents for electroless copper deposition was documented by Vaskelis with co-workers in 1995 [19]. The authors carried out detailed investigations on the behavior of the Co^{3+} - Co^{2+} -ethylenediamine redox couple in systems related to electroless copper deposition [20–28]. Ethylenediamine as a ligand is not an exclusive amine for Co^{3+} - Co^{2+} redox couples in the electroless copper plating systems. Co^{2+} complexes with other higher polyamines, e.g., propylene diamine (propane-1,2-diamine) [29,30], diethylenetriamine [31,32], or pentaethylenhexamine [33], and are eligible reducing agents to reduce Cu^{2+} to the metallic state on a surface to be plated.

It is worth noting that Co^{2+} complexes with different amines have found application as reducing agents for electroless deposition of metals different from Cu. The authors successfully used the Co^{3+} - Co^{2+} -ammonia redox couple for the deposition of silver coatings [34,35]. Electroless gold plating was carried out when using trimethylene diamine as a Co^{2+} ligand [29]. Electroless deposition of platinum using Co^{2+} complexes with diethylenetriamine as a reducing agent was documented recently [36].

In this work, we investigated autocatalytic reduction of Pt^{4+} by the Co^{3+} - Co^{2+} -diethylenetriamine redox couple. The Co^{2+} metal ion reducing agent-containing bath is operable below room temperature and with a low pH. Additionally, the kinetics of electroless deposition of platinum have been investigated using electrochemical quartz crystal microgravimetry (EQCM). The method is based on the Sauerbrey's equation [37], where the measured frequency changes of the quartz crystal are correlated with the mass changes according to Equation (4):

$$\Delta f = -2 \frac{f_0^2 \Delta m}{S \sqrt{\mu_q \rho_q}} \quad (4)$$

where f_0 —is the resonant frequency of the quartz crystal, S is the piezoelectrically active area (cm^2), μ_q is the shear modulus of the quartz ($2.947 \cdot 10^{11} \text{ g cm}^{-1} \text{ s}^{-2}$) and ρ_q is its density (2.648 g cm^{-3}) [38]. As seen from Equation (5),

$$\Delta m = -\Delta f S C_q \quad (5)$$

where C_q —the quartz crystal sensitivity constant. For a 6 MHz quartz crystal, it is $12.26 \text{ ng cm}^{-2} \text{ Hz}^{-1}$. This sensitive method allows determining small in situ changes in the electrode mass, which are directly proportional to the changes in the quartz crystal resonant frequency.

2. Materials and Methods

Electroless Pt films were deposited onto a roughed glass sheet (1 cm · 2.5 cm) at a temperature of 20 °C. The surface roughness factor of the glass sheet was ca. 10. The scheme of electroless Pt deposition is shown in Figure 1. At first, the roughed glass sheet's cleaning procedure (the same in all experiments) was carried out by degreasing the glass sheet in a $\text{K}_2\text{Cr}_2\text{O}_7 + \text{H}_2\text{SO}_4$ solution. After that, the glass sheet was sensitized in a $1 \text{ g L}^{-1} \text{ SnCl}_2$ solution for 1 min, rinsed with distilled water, then activated in a $1 \text{ g L}^{-1} \text{ PdCl}_2$ solution for 1 min, rinsed with deionized water, and then immersed into the electroless Pt plating bath.

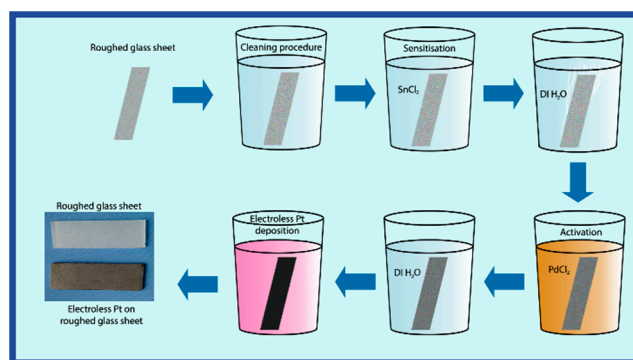


Figure 1. Scheme of electroless platinum deposition.

The electroless Pt plating bath containing $0.004\text{--}0.012\text{ mol L}^{-1}$ H_2PtCl_6 , 0.4 mol L^{-1} NH_4OH , and 0.16 mol L^{-1} diethylenetriamine (dien) was prepared. The addition of HCl adjusted the solution pH to 7.5. It is well-known that the Co^{2+} compounds react with oxygen in alkaline solutions [39]. The plating solution was deaerated with argon (Ar) for 10 min to remove the oxygen. Then, the required amount of CoCl_2 in the range of $0\text{--}0.25\text{ mol L}^{-1}$ was added to the electroless plating solution. Later studies of Pt deposition were carried out in the deaerated solution with continuous Ar bubbling through the solution. The main experiments were performed at a temperature of $20\text{ }^\circ\text{C}$ and the time (t_{dep}) of electroless Pt deposition was 30 min unless otherwise stated.

A SEM/FIB workstation Helios Nanolab 650 (FEL, Eindhoven, The Netherlands) with an energy dispersive X-ray (EDX) spectrometer INCA Energy 350 XMax 20 (Oxford Instruments, Abingdon, UK) was used to investigate the morphology of the Pt films deposited on the surface of a glass sheet.

A tearing fastness test was used to evaluate the adhesion strength of the deposited Pt layer on a roughed glass sheet. Briefly, the tearing fastness test was performed by pasting tape on Pt coating's surface and then tearing the tape off quickly to observe the surface peeling condition of the Pt layer.

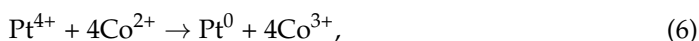
Electrochemical quartz crystal microgravimetry (EQCM) was used to investigate the kinetics of electroless deposition of Pt films. EQCM setup is described in detail in Reference [40].

Before the electroless platinum deposition measurements, a copper layer was electrodeposited on a gold sublayer onto quartz crystals installed at the bottom of the cell from a solution containing 1.0 mol L^{-1} CuSO_4 and 0.5 mol L^{-1} H_2SO_4 at a current of 10 mA for 1 min. Initially, the instantaneous rate of electroless Pt deposition was determined on the electrodeposited copper surface.

For comparison, the EQCM experiments were carried out in two ways: (i) the deposition of Pt was investigated, then the prepared and deaerated Pt plating solution was not bubbled (agitated) with Ar (denoted as “without Ar bubbling”) during the deposition process; and (ii) the electroless Pt plating solution was bubbled with Ar during the deposition process (denoted as “with Ar bubbling”).

3. Results

Electroless Pt films were deposited on the surface of a roughed glass sheet using the $\text{Co}^{3+}/\text{Co}^{2+}$ ions couple as a reducing agent and diethylenetriamine as a complexing agent. Generally, the reduction of Pt^{4+} with Co^{2+} in diethylenetriamine solutions occurs as follows:



and it is the sum of two (anodic and cathodic) partial reactions, simultaneously occurring on the surface to be plated:





Figure 2 presents the dependence of Pt deposition rate on solution pH. Formation of Pt coatings begins at a pH over 6.5 (Figure 2). A sharp increase in the amount of deposited Pt is observed when pH rises from 6.5 to 7.5. The maximum plating rate obtained was close to 0.09 mg cm^{-2} for 30 min. With further pH increment, the plating rate remains constant or slightly diminishes (Figure 2). It is worth noting that creating the solutions with a pH higher than 8.5 was impossible due to a precipitate formation.

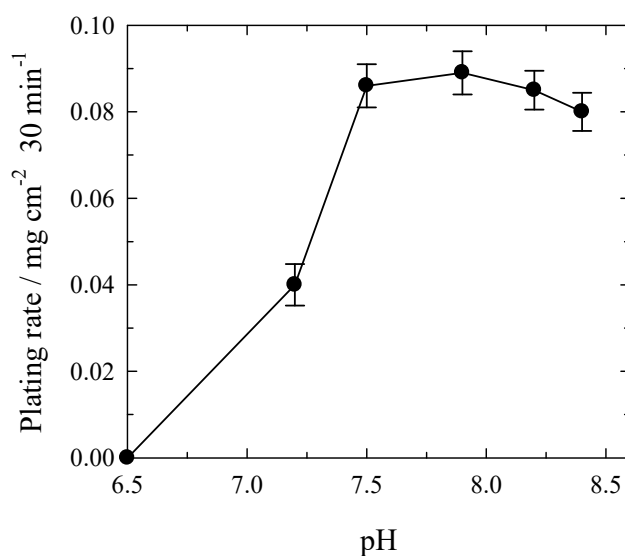


Figure 2. Dependence of plating rate of Pt on the solution pH under conditions with Ar bubbling. Solution contained (mol L^{-1}): H_2PtCl_6 —0.004; NH_4OH —0.4; complexing agent—0.16; CoCl_2 —0.2; HCl to $\text{pH} = 7.5$; $t_{\text{dep}} = 30 \text{ min}$; $20 \text{ }^\circ\text{C}$.

The dependence of deposited Pt mass on a roughed glass sheet plating time is shown in Figure 3. As evident, the mass of deposited Pt film increases with time. During the first 30 min, the observed deposition rate is the highest, whereas later, it slows down and stops after 2 h (Figure 3). It should be noted that Pt deposits of 0.12 mg cm^{-2} during 90 min can be obtained from the solutions investigated without additional replenishment of the reactants (Figure 3). The decrease in Pt deposition rate can be explained by the formation, accumulation, and adsorption of the reaction products (e.g., Co^{3+} -dien complexes) on the surface to be plated, which diminishes the Pt catalytic surface. The same phenomenon was observed in electroless copper plating using $\text{Co}^{3+}/\text{Co}^{2+}$ -ethylenediamine complexes as a reducing agent [26]. The authors investigated the copper deposition under unstirred and hydrodynamic conditions. As the jet of electrolyte removes inhibiting Co^{3+} species from the surface and ensures the transport of both reacting species (Co^{2+} and Cu^{2+}) to the electrode, the copper deposition rate was ca. 10 times higher compared with that under stationary conditions.

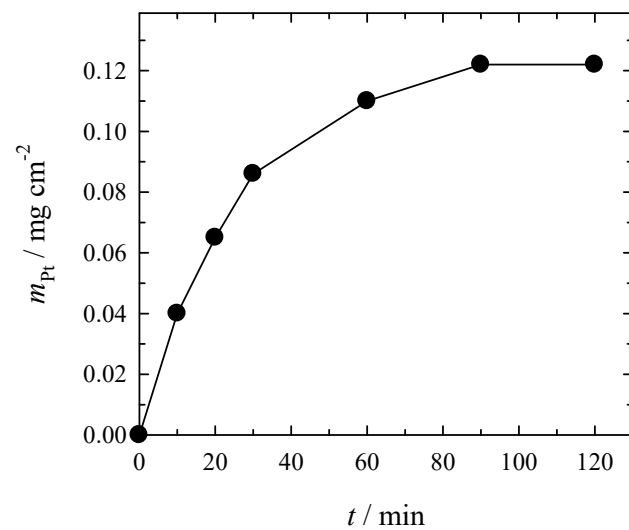


Figure 3. Dependence of deposited Pt mass on the roughed glass sheet on time under conditions with Ar bubbling. The solution composition is the same as in Figure 2.

At a constant Pt^{4+} concentration, the platinum plating rate increases with the rise in Co^{2+} concentration (Figure 4). The concentration dependence has a distinctly expressed maximum at 0.2 mol L^{-1} of Co^{2+} , and the highest Pt deposition rate was found to be ca. 0.09 mg cm^{-2} during 30 min and the thickness being ca. $0.05 \mu\text{m}$. A further increase in Co^{2+} concentration results in the slowdown of the platinum plating rate.

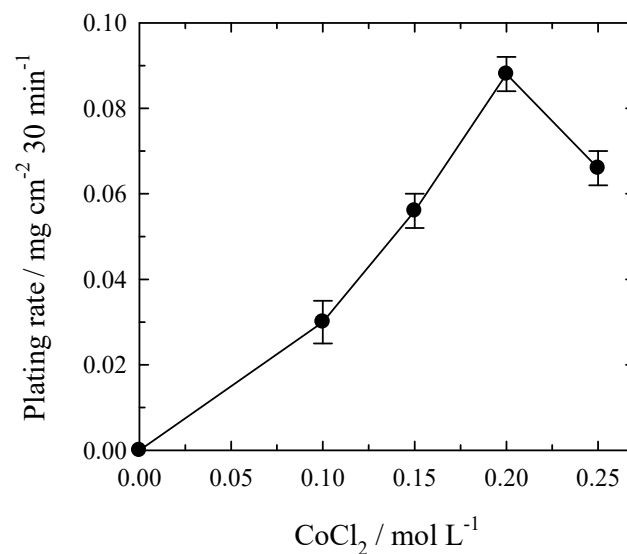


Figure 4. Effect of Co^{2+} concentration on the rate of electroless Pt plating under deaeration with Ar. Solution composition (mol L^{-1}): H_2PtCl_6 —0.004; NH_4OH —0.4; complexing agent—0.16; HCl to pH = 7.5; $t_{\text{dep}} = 30 \text{ min}$; $20 \text{ }^\circ\text{C}$.

Under conditions of constant Co^{2+} concentration, the mass of deposited platinum depends practically linearly on the concentration of Pt^{4+} in the concentration range investigated (Figure 5a). In Figure 5b, natural logarithmic plating rates of Pt vs. natural logarithmic bulk concentrations of H_2PtCl_6 were plotted. The slope of the straight line is 0.9852, indicating 1st order kinetics. The maximum electroless platinum deposition rate is ca. 0.27 mg cm^{-2} during 30 min and is observed at a concentration of Pt^{4+} equal to 0.012 mol L^{-1} (Figure 5a). The thickness of the deposited Pt layer was ca. $0.13 \mu\text{m}$.

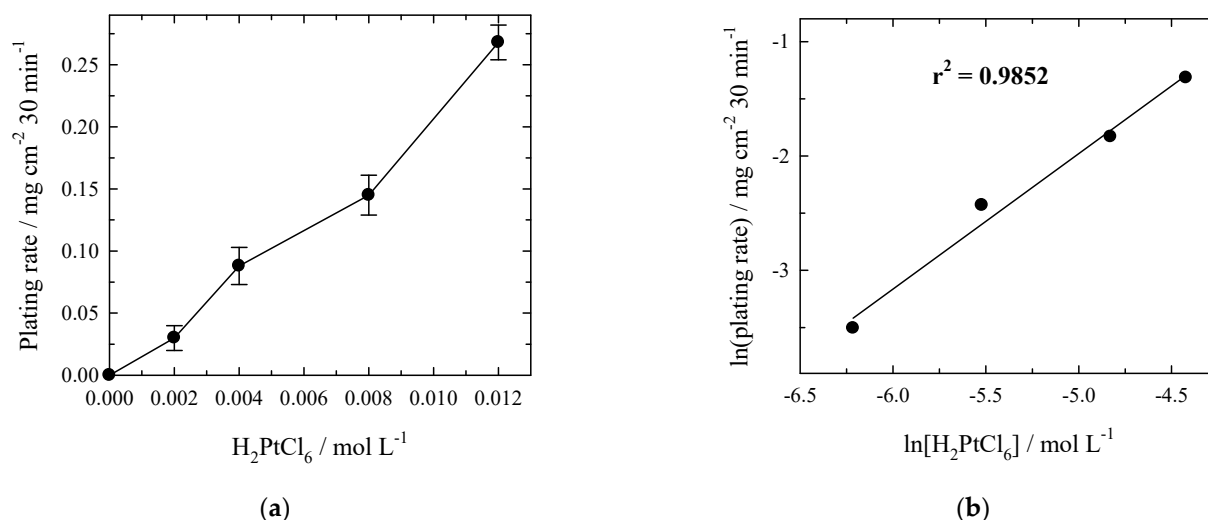


Figure 5. (a) Effect of Pt⁴⁺ concentration on the rate of electroless Pt plating under conditions with Ar bubbling. Solution composition (mol L⁻¹): CoCl₂—0.2; NH₄OH—0.4; complexing agent—0.16; HCl to pH = 7.5; $t_{\text{dep}} = 30$ min; 20 °C. (b) Dependence of natural logarithmic plating rates of Pt vs. natural logarithmic bulk concentrations of H₂PtCl₆.

The electroless Pt deposition begins at a relatively low temperature (5 °C) and increases up to a distinct maximum value of the temperature, equal to 15–17 °C (Figure 6a). After the increase in temperature from 17 to 50 °C, the platinum plating rate unexpectedly decreases more than fivefold. Interestingly, the platinum deposition rate at a temperature of 50 °C is twice as low as that at 5 °C (Figure 6a). The decrease in Pt plating rate at temperatures higher than 15 °C may be attributed to the changes in solution equilibria at higher temperatures or/and the surface contamination by reaction products formed at higher temperatures. The Arrhenius plot was calculated from the first three points and given in Figure 6b. The activation energy is ca. 52 kJ mol⁻¹.

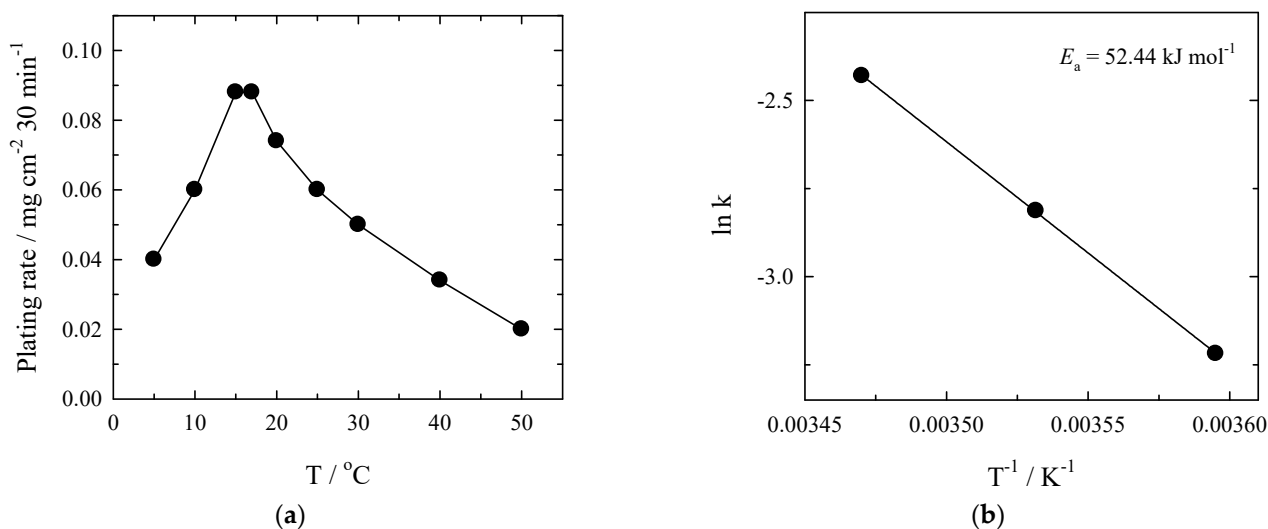


Figure 6. (a) Effect of temperature on the rate of electroless Pt plating under conditions with Ar bubbling. The solution composition is the same as in Figure 2. (b) The Arrhenius plot calculated from Pt deposition rates for the first three points in the same solution.

Therefore, based on the data obtained, we can conclude that the optimum operating conditions (high enough plating rate and moderate temperature) are as follows (mol L⁻¹): H₂PtCl₆—0.004; CoCl₂—0.2; NH₄OH—0.4; complexing agent—0.16; pH = 7.5, the temperature being 17–20 °C. Experiments showed that the Pt films with a thickness greater than

0.1 mg cm⁻² could be obtained on the surface of the glass sheet without replenishment of the solution (Figure 3). The solutions were stable during the electroless Pt deposition, and the reduction of Pt⁴⁺ occurred only on the surface plated, no considerable signs of the reduction of Pt⁴⁺ in the solution bulk were observed.

For comparison, the Pt coating was deposited on the roughed glass sheet using the conventional electroless Pt plating bath described in Reference [1]. The bath contained 0.03 M Na₂Pt(OH)₆, 0.12 M ethylenediamine, 0.125 M NaOH, and 0.02 M N₂H₄. The solution pH was ~10, the operating temperature was 35 °C. Figure 7 presents the rate of Pt deposition using the Co³⁺/Co²⁺ redox couple and N₂H₄ as reducing agents. In the case of Pt plating bath with N₂H₄, the reduction of Pt⁴⁺ occurs in the solution bulk after one h of deposition, indicating the plating solution instability. Comparing the electroless Pt plating process using the Co³⁺/Co²⁺ redox couple and N₂H₄ as reducing agents shows the advantages of Co²⁺ complexes as reducing agents. The rate of Pt plating using the Co³⁺/Co²⁺ redox couple as a reducing agent is ca. 3 times higher than that using N₂H₄ as a reducing agent. Furthermore, the solution stability of Pt plating bath with Co²⁺ complexes is much better than that with N₂H₄ (Figure 7).

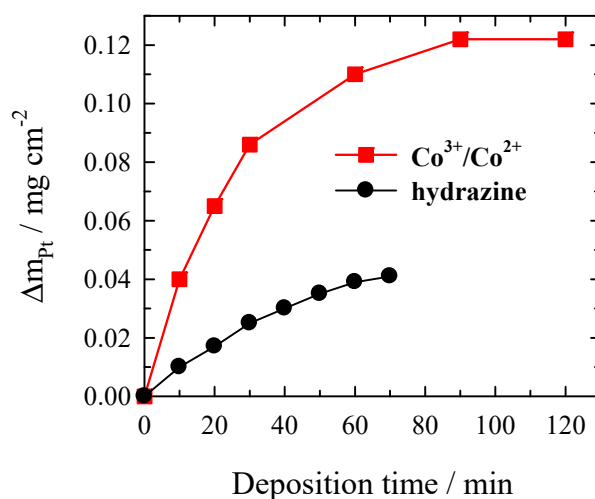


Figure 7. The rate of Pt deposition using different reducing agents.

Figure 8 presents the electrolessly deposited Pt coatings SEM views, obtained using the Co²⁺ complexes (a) and hydrazine (b) as reducing agents. It is seen that in the case of hydrazine, the coating is built from much larger Pt conglomerates, comparing with that using the Co²⁺ complexes as a reducing agent (Figure 8). As seen, the Pt film obtained is compact and of good quality (Figure 8a). Concerning the adhesion of Pt coatings received using Co³⁺/Co²⁺ and N₂H₄ as reducing agents, it can be noted that the adhesion of the coating is higher enough. The tearing test showed no surface peeling for the deposited Pt coatings, indicating a strong adhesion of Pt coatings with a roughed glass sheet.

The electroless deposition of Pt was investigated in more detail employing electrochemical quartz crystal microbalance. The instantaneous rate of Pt deposition on the initial electroplated copper surface was investigated in solutions, which were deaerated with Ar before the measurements, and during the deposition of Pt, those solutions were not bubbled with Ar, and in solutions under conditions of constant Ar bubbling during the deposition process. The EQCM data on the electroless Pt deposition using the Co³⁺/Co²⁺ redox couple as a reducing agent are shown in Figure 9, which presents the main measured parameters of the electroless Pt deposition: open-circuit potential (a), change in frequency (b), and Pt mass gain (c).

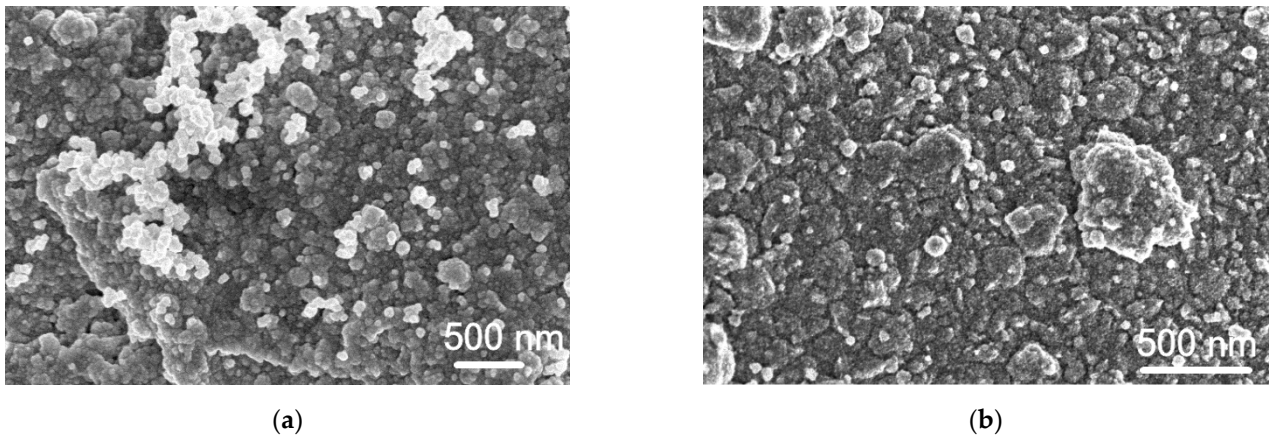


Figure 8. SEM images of the roughed glass sheet after the electroless Pt plating using the $\text{Co}^{3+}/\text{Co}^{2+}$ redox couple (a) and hydrazine (b) as reducing agents.

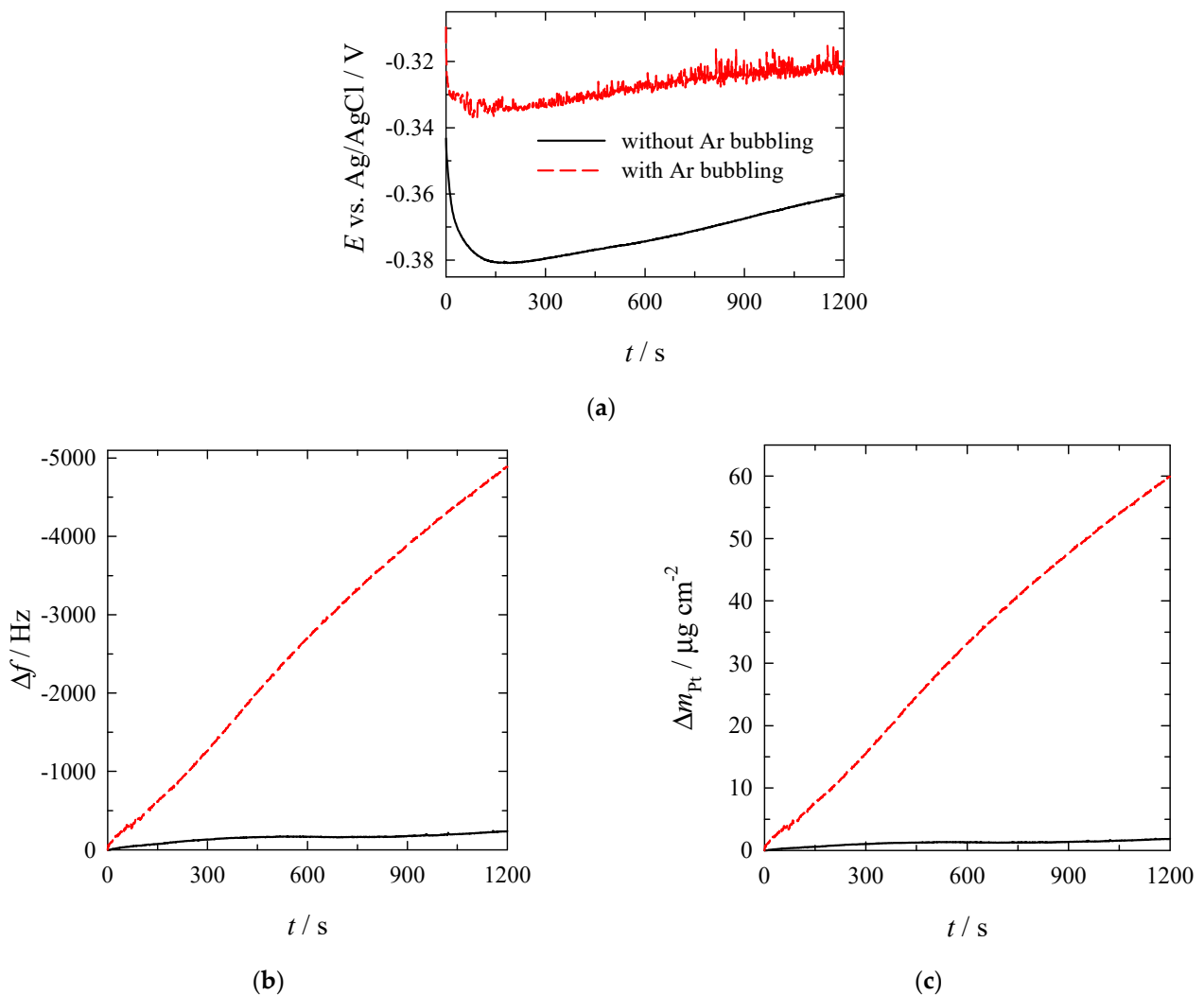


Figure 9. Kinetics of electroless platinum plating under conditions with Ar bubbling (dashed line) and deaerated and not-agitated solution (solid line) under stationary conditions: open-circuit potential (a), change in frequency (b) and platinum mass gain (c). Solution contained (mol L^{-1}): H_2PtCl_6 —0.004; NH_4OH —0.4; complexing agent—0.16; CoCl_2 —0.2; HCl to pH = 7.5; 20 °C.

It is evident that in the absence of an external current, the electrode attains a mixed potential (E_m) value (Figure 9a). The open-circuit potential of Cu in the course of electroless deposition is quite stable during the electroless Pt deposition under both conditions, while its values after ca. 150 s slightly shift to more positive values (Figure 9a). During the electroless Pt deposition, the frequency begins to decrease, i.e., the coating mass increases linearly with time (Figure 9b,c). Moreover, the bubbling of the electroless Pt plating solution with argon results in a higher Pt deposition rate. The rate of the electroless Pt deposition under bubbling with argon is ca. $3 \mu\text{g cm}^{-2} \text{min}^{-1}$, whereas the value of plating rate of $0.14 \mu\text{g cm}^{-2} \text{min}^{-1}$ was determined in the solution that was not bubbled during deposition. Notably, under conditions of bubbling with Ar, the Pt films with a thickness greater than $60 \mu\text{g cm}^{-2}$ may be obtained without replenishing the solution over 20 min (Figure 8c).

4. Conclusions

The kinetics of electroless deposition of Pt on a roughed glass sheet, using the cobalt ion redox system ($\text{Co}^{3+}/\text{Co}^{2+}$) as a reducing agent, has been investigated. It has been determined that the deposition of Pt depends on pH, the concentration of reactants, temperature, and the agitation of the plating solution by bubbling with Ar. It was found that the Pt films with a thickness greater than 0.11 mg cm^{-2} could be obtained on the surface of the roughed glass sheet without replenishment of the solution over one h.

The electroless deposition of Pt on the Cu electrode has been investigated using electrochemical quartz crystal microbalance. The agitation of the electroless Pt plating solution by bubbling with argon results in higher deposition rates of Pt—the rate of the electroless Pt deposition is ca. $3 \mu\text{g cm}^{-2} \text{min}^{-1}$. In the case of the non-agitated plating solution, the rate of Pt deposition is significantly lower, e.g., $0.14 \mu\text{g cm}^{-2} \text{min}^{-1}$. The Pt films obtained are compact and of good quality.

Author Contributions: This study was conducted through the contributions of all authors. Conceptualization L.T.-T. and E.N.; methodology, A.J., I.S. and A.N.; investigation, A.J., I.S., L.T. and L.M.; data curation, L.T., L.M. and A.N.; writing—original draft preparation, L.T.-T. and E.N.; writing—review and editing, Y.D. and V.B.; visualization, Y.D. and V.B. All authors have read and agreed to the published version of the manuscript.

Funding: This research was funded by the Research Council of Lithuania (LMTLT), grant number TEC-06/2015.

Institutional Review Board Statement: Not applicable.

Informed Consent Statement: Not applicable.

Conflicts of Interest: The authors declare no conflict of interest.

References

1. Duflek, E.F.; Baudrand, D.W.; Donaldson, J.G. Electronic Applications of Electroless Nickel. In *Electroless Plating: Fundamentals and Applications*; Mallory, G.O., Hajdu, J.B., Eds.; American Electroplaters and Surface Finishers Society: Orlando, FL, USA, 1990.
2. Okinaka, Y.; Osaka, T. *Advances in Electrochemical Science and Engineering*; Gerischer, H., Tobias, C.W., Eds.; VCH Publishers: Weinheim, Germany, 1994; Volume 3.
3. Vaškelis, A. *Coatings Technology Handbook*, 2nd ed.; Satas, D., Tracton, A.A., Eds.; Marcel Dekker: New York, NY, USA, 2001; p. 213.
4. O'Sullivan, E.J. Fundamental and Practical Aspects of the Electroless Deposition Reaction. In *Advances in Electrochemical Science and Engineering*; Alkire, R.C., Kolb, D.M., Eds.; Wiley-VCH: Weinheim, Germany, 2002; Volume 7, pp. 225–273. [[CrossRef](#)]
5. Djokić, S.S.; Cavallotti, P.L. *Modern Aspects of Electrochemistry, Electroless Deposition: Theory and Applications*; Djokić, S.S., Ed.; Springer: New York, NY, USA, 2010; Volume 48, pp. 251–289.
6. Mustain, W.E.; Kim, H.; Narayanan, V.; Osborn, T.; Kohl, P.A. Electroless deposition and characterization of $\text{Pt}_x\text{Ru}_{1-x}$ catalysts on Pt/C nanoparticles for methanol oxidation. *J. Fuel Cell Sci. Technol.* **2010**, *7*, 041013. [[CrossRef](#)]
7. Wongkaew, L.A.; Zhang, Y.; Tengco, J.M.M.; Blom, D.A.; Sivasubramanian, P.; Fanson, P.T.; Regalbutto, J.R.; Monnier, J.R. Characterization and evaluation of Pt-Pd electrocatalysts prepared by electroless deposition. *Appl. Catal. B Environ.* **2016**, *188*, 367–375. [[CrossRef](#)]
8. Tate, G.; Kevin, A.; Diao, W.; Monnier, J.R. Preparation of Pt-containing bimetallic and trimetallic catalysts using continuous electroless deposition methods. *Catal. Today* **2019**, *334*, 113–121. [[CrossRef](#)]

9. Egelske, B.T.; Keels, J.M.; Monnier, J.R.; Regalbutto, J.R. An analysis of electroless deposition derived Ni-Pt catalysts for the dry reforming of methane. *J. Catal.* **2020**, *381*, 374–384. [[CrossRef](#)]
10. Wagner, C.; Traud, W. Zeitschrift fur Elektrochemie und Angewandte physikalische Chemie. *Z. Elektrochem.* **1938**, *44*, 391–454. [[CrossRef](#)]
11. Saito, M. Electrode oxidation reaction of formaldehyde. *J. Met. Fin. Soc. Jpn.* **1965**, *16*, 300–305. [[CrossRef](#)]
12. Paunovic, M. Electrochemical aspects of electroless deposition of metals. *Plating* **1968**, *55*, 1161–1167.
13. Spiro, M. Heterogeneous catalysis in solution. Part 17.—Kinetics of oxidation–reduction reaction catalysed by electron transfer through the solid: An electrochemical treatment. *J. Chem. Soc. Faraday Trans.* **1979**, *75*, 1507–1512. [[CrossRef](#)]
14. Vitry, V.; Bonin, L. Increase of boron content in electroless nickel-boron coating by modification of plating conditions. *Surf. Coat. Technol.* **2017**, *311*, 164–171. [[CrossRef](#)]
15. Bonin, L.; Castro, C.C.; Vitry, V.; Hantson, A.-L.; Delaunois, F. Optimization of electroless NiB deposition without stabilizer, based on surface roughness and plating rate. *J. Alloys Comp.* **2018**, *767*, 276–284. [[CrossRef](#)]
16. Algul, H.; Uysal, M.; Alp, A. A comparative study on morphological, mechanical and tribological properties of electroless NiP, NiB and NiBP coatings. *Appl. Surf. Sci. Adv.* **2021**, *4*, 100089. [[CrossRef](#)]
17. Zhang, Y.; Yan, Z.; Zhang, M.; Tan, Y.; Jia, S.; Liu, A. Green electroless plating of cuprous oxide nanoparticles onto carbon nanotubes as efficient electrocatalysts for hydrogen evolution reaction. *Appl. Surf. Sci.* **2021**, *548*, 149218. [[CrossRef](#)]
18. Zhang, B. Green Electroless Plating. In *Amorphous and Nano Alloys Electroless Depositions*; Elsevier Inc.: Amsterdam, The Netherlands, 2016; pp. 583–627. [[CrossRef](#)]
19. Vaškelis, A.; Jačiauskienė, J.; Norkus, E. The kinetics of autocatalytic Cu (II) reduction by Co (II) complexes. *Chemija* **1995**, *3*, 16.
20. Vaškelis, A.; Norkus, E.; Rozovskis, G.; Vinkevičius, H.J. New methods of electroless plating and direct electroplating of plastics. *Trans. IMF* **1997**, *75*, 1–3. [[CrossRef](#)]
21. Jusys, Z.; Stalnionis, G. Autocatalytic reduction of Cu(II) to copper by Co(II) studied by electrochemical quartz crystal microgravimetry in a wall jet cell. *J. Electroanal. Chem.* **1997**, *431*, 141–144. [[CrossRef](#)]
22. Vaškelis, A.; Norkus, E.; Reklaitis, J.; Jačiauskienė, J. Electroless copper plating using cobalt(II)-ethylenediamine complex compounds as reducing agents: 1. The thermodynamical aspects. *Chemija* **1998**, *3*, 199–205.
23. Norkus, E.; Vaškelis, A.; Jačiauskienė, J. Electroless copper plating using cobalt(II)-ethylenediamine complex compounds as reducing agents: 2. A kinetic study. *Chemija* **1998**, *4*, 284–290.
24. Vaškelis, A.; Norkus, E. Autocatalytic processes of copper(II) and silver(I) reduction by cobalt(II) complexes. *Electrochim. Acta* **1999**, *44*, 3667–3677. [[CrossRef](#)]
25. Vaškelis, A.; Norkus, E.; Jačiauskienė, J.; Reklaitis, J. Stromlose Verkupferung mit Kobalt(II)-Ethylenediamin-Komplexverbindungen als Reduktionsmittel. Thermodynamische Aspekte und kinetische Untersuchungen. *Galvanotechnik* **1999**, *90*, 1556–1569.
26. Vaškelis, A.; Stalnionis, G.; Jusys, Z. Cyclic voltammetry and quartz crystal microgravimetry study of autocatalytic copper(II) reduction by cobalt(II) in ethylenediamine solutions. *J. Electroanal. Chem.* **1999**, *465*, 142–152. [[CrossRef](#)]
27. Jusys, Z.; Stalnionis, G. Wall-jet electrochemical quartz crystal microgravimetry: Oxidation of Co(II)–ethylenediamine complexes on copper electrode. *Electrochim. Acta* **2000**, *45*, 3675–3682. [[CrossRef](#)]
28. Vaškelis, A.; Norkus, E.; Jačiauskienė, J. Kinetics of electroless copper deposition using cobalt(II)-ethylenediamine complex compounds as reducing agents. *J. Appl. Electrochem.* **2002**, *32*, 297–303. [[CrossRef](#)]
29. Vaškelis, A.; Jačiauskienė, J.; Jagminienė, A.; Norkus, E. Obtaining of IB group metal films by novel electroless deposition method. *Solid State Sci.* **2002**, *4*, 1299–1304. [[CrossRef](#)]
30. Dordi, Y.; Thie, W.; Vaškelis, A.; Norkus, E.; Jačiauskienė, A.; Jagminienė, A. Plating Solutions for Electroless Deposition of Copper. U.S. Patent US7297190B1, 20 November 2007.
31. Vaškelis, A.; Norkus, E.; Jačiauskienė, A.; Jagminienė, A. Plating Solution for Electroless Deposition of Copper. U.S. Patent US7306662B2, 11 December 2007.
32. Vaškelis, A.; Stankevičienė, I.; Jagminienė, A.; Tamašauskaitė-Tamašiūnaitė, L.; Norkus, E. The autocatalytic reduction of copper(II) by cobalt(II) in aqueous diethylenetriamine solutions studied by EQCM. *J. Electroanal. Chem.* **2008**, *622*, 136–144. [[CrossRef](#)]
33. Norkus, E.; Stankevičienė, I.; Tamašauskaitė-Tamašiūnaitė, L.; Stalnionis, G.; Prušinskas, K.; Jagminienė, A. EQCM and CV study of autocatalytic copper(II) reduction by cobalt(II) pentaethylenhexamine complexes in wide pH range. *J. Electrochem. Soc.* **2014**, *161*, D373–D380. [[CrossRef](#)]
34. Vaškelis, A.; Jagminienė, A.; Juškėnas, R.; Matulionis, E.; Norkus, E. Structure of electroless silver coatings obtained using cobalt(II) as reducing agent. *Surf. Coat. Technol.* **1996**, *82*, 165–168. [[CrossRef](#)]
35. Norkus, E.; Vaškelis, A.; Jagminienė, A.; Tamašauskaitė-Tamašiūnaitė, L. Kinetics of electroless deposition using cobalt(II)-ammonia complex compounds as reducing agents. *J. Appl. Electrochem.* **2001**, *31*, 1061–1066. [[CrossRef](#)]
36. Norkus, E.; Stankevičienė, I.; Jagminienė, A.; Tamašauskaitė-Tamašiūnaitė, L.; Joi, A.; Dordi, Y. Electroless Deposition of Continuous Platinum Layer Using Complexed Co²⁺ Metal Ion Reducing Agent. U.S. Patent US9499913B2, 22 November 2016.
37. Sauerbrey, G.Z. The use of quartz oscillators for weighing thin layers and for microweighing. *Z. Phys.* **1959**, *155*, 206–222. [[CrossRef](#)]
38. Buttry, D.A.; Ward, M.D. Measurement of interfacial processes at electrode surfaces with the electrochemical quartz crystal microbalance. *Chem. Rev.* **1992**, *92*, 1355–1379. [[CrossRef](#)]

-
39. Norkus, E.; Vaškelis, A.; Grigucevičienė, A.; Rozovskis, G.; Reklaitis, J.; Norkus, P. Oxidation of cobalt(II) with air oxygen in aqueous ethylenediamine solutions. *Trans. Met. Chem.* **2001**, *26*, 465–472. [[CrossRef](#)]
 40. Norkus, E.; Stankevičienė, I.; Tamašauskaitė-Tamašiūnaitė, L.; Prušinskas, K. Comparative study of electroless copper deposition using different cobalt(II)-amine complex compounds as reducing agents. *Chemija* **2012**, *23*, 1–6.